

Pyroelectric properties of $91.5\text{Na}_{0.5}\text{Bi}_{0.5}\text{TiO}_3\text{-}8.5\text{K}_{0.5}\text{Bi}_{0.5}\text{TiO}_3$ lead-free single crystal

Bo Zhang*, Renbing Sun*[‡], Fang Wang*, Tangfu Feng*,
Pengna Zhang* and Haosu Luo[†]

*School of Materials and Chemical Engineering
Ningbo University of Technology
Ningbo, Zhejiang 315016, P. R. China

[†]Key Laboratory of Inorganic Functional Materials and Devices
Shanghai Institute of Ceramics, Chinese Academy of Sciences
Jiading, Shanghai 201800, P. R. China

[‡]renbingsun@hotmail.com

Received 7 May 2021; Revised 6 August 2021; Accepted 12 August 2021; Published 10 November 2021

The dielectric and pyroelectric performances of $91.5\text{Na}_{0.5}\text{Bi}_{0.5}\text{TiO}_3\text{-}8.5\text{K}_{0.5}\text{Bi}_{0.5}\text{TiO}_3$ lead-free single crystal were investigated. The depolarization temperature of the crystal is about 153 °C. Among the $\langle 001 \rangle$, $\langle 110 \rangle$, and $\langle 111 \rangle$ crystallographic orientations, the $\langle 111 \rangle$ -oriented crystal possesses the highest pyroelectric coefficient and the largest figures of merit, and the values of p , F_v , and F_d are $5.63 \times 10^{-4} \text{ C/m}^2 \cdot \text{K}$, $0.06 \text{ m}^2/\text{C}$, and $21.5 \mu\text{Pa}^{-1/2}$ for the $\langle 111 \rangle$ -oriented crystal at room temperature. The F_d and F_v exhibit weak frequency dependence in the range of 100–300 Hz. With the increase of the temperature, the value of p increases, while the value of F_v decreases from 18 °C to 103 °C.

Keywords: Lead-free; single crystal; pyroelectric properties; dielectric properties.

1. Introduction

At present, lead zirconate titanate (PZT) family-based materials are the most practical pyroelectric and piezoelectric materials due to their outstanding electrical properties. However, the content of lead is as high as 60%. Serious lead pollution has become a key problem restricting the development of electrical materials industry. In recent years, with the improvement of people's health and environmental awareness, the investigation of lead-free materials has rapidly become a research hotspot. For example, $\text{Bi}_{0.5}\text{Na}_{0.5}\text{TiO}_3$ -based, $\text{K}_{0.5}\text{Na}_{0.5}\text{NbO}_3$ -based, and $\text{Ba}(\text{Ti}_{0.8}\text{Zr}_{0.2})\text{O}_3\text{-}(\text{Ba}_{0.7}\text{Ca}_{0.3})\text{TiO}_3$ -based lead-free materials are widely investigated.^{1–9} Among these lead-free materials, lead-free single crystal materials, such as $\text{Bi}_{0.5}\text{Na}_{0.5}\text{TiO}_3\text{-BaTiO}_3$, $\text{Bi}_{0.5}\text{Na}_{0.5}\text{TiO}_3\text{-Bi}_{0.5}\text{K}_{0.5}\text{TiO}_3$, and $\text{K}_{0.5}\text{Na}_{0.5}\text{NbO}_3$ single crystals,^{3–5} have attracted more attention because of their outstanding electrical properties. For these lead-free single crystal materials, there are more studies on the dielectric, ferroelectric, and piezoelectric properties, but their pyroelectric properties have been less studied.

In this paper, orientation dependences of pyroelectric and dielectric properties along with the temperature dependences

of $91.5\text{Na}_{0.5}\text{Bi}_{0.5}\text{TiO}_3\text{-}8.5\text{K}_{0.5}\text{Bi}_{0.5}\text{TiO}_3$ (91.5NBT–8.5KBT) lead-free single crystal were investigated in detail.

2. Experimental Procedure

The 91.5NBT–8.5KBT single crystal was grown by the top-seeded solution growth (TSSG) method. The chemical materials of Na_2CO_3 , Bi_2O_3 , TiO_2 , and K_2CO_3 with purities of 99.90% were used as the raw materials. The details of the growth process were similar to those of the $\text{Na}_{0.5}\text{Bi}_{0.5}\text{TiO}_3\text{-Na}_{0.5}\text{Bi}_{0.5}\text{TiO}_3$ single crystal growth.⁴ X-ray powder diffraction (XRPD) measurement was carried out to check the lattice structure. Inductively Coupled Plasma Atomic Emission Spectrometry (ICP-AES) was used to measure the concentration of K. The $\langle 001 \rangle$ -, $\langle 110 \rangle$ -, and $\langle 111 \rangle$ -direction crystal wafers were cut into $3 \times 3 \times 0.5\text{-mm}^3$ size for specific heat per unit mass, pyroelectric, and dielectric properties characterization. The silver electrodes were fired on both sides at 800 °C after these crystal wafers were polished with Al_2O_3 powders. These samples were poled under a DC electric field of 3 kV/mm for 15 min in silicon oil. The pyroelectric coefficient was measured by a dynamic technique

[‡]Corresponding author.

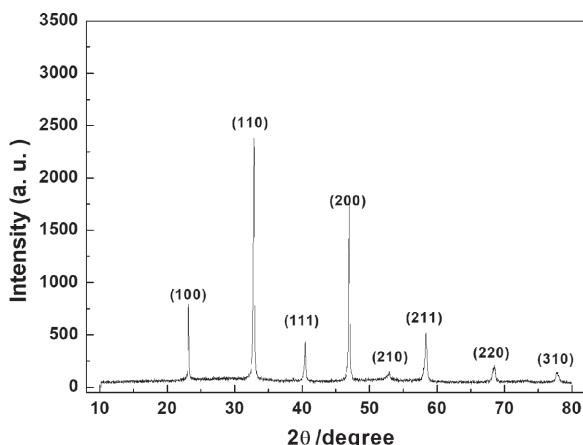


Fig. 1. XRPD patterns of 91.5NBT–8.5KBT single crystal.

using sinusoidal temperature change with an amplitude of 0.25 °C at a frequency of 45 mHz.¹⁰

3. Results and Discussion

3.1. Crystal structure

The concentration of K-ion in the as-grown single crystal is 8.5 at.%, measured by ICP-AES. The XRPD patterns are shown in Fig. 1. All the diffraction reflections exhibit sharp and symmetric single diffraction peaks with rhombohedral symmetry (pseudocubic phase). So the as-grown crystal exists in pure rhombohedral perovskite structure. The unit-cell parameters are $a = b = c = 3.8949 \text{ \AA}$ and $\alpha = \beta = \gamma = 90.037 \text{ \AA}$, which are calculated based on the XRPD data.

3.2. Dielectric properties

The temperature dependences of dielectric constant and dielectric loss for <001>-, <110>-, and <111>-oriented poled 91.5NBT–8.5KBT crystals are shown in Fig. 2, which were measured at 1 kHz. The (T_m, ε_m) values for <001>-, <110>-, and <111>-oriented poled crystals are (318 °C, 4868), (319 °C, 2909), and (317 °C, 1348), respectively. The T_m is almost independent of crystal orientations. However, the difference of ε_m for the three crystallographic orientation crystals is large, which indicates the crystal shows obvious anisotropy. There are two distinct dielectric anomalies in the $\varepsilon(T)$ curves, which are related to two phase transitions. According to Refs. 11 and 12, the maximum permittivity peak at about 318 °C relates to the $Pnma$ orthorhombic–tetragonal phase transition, while a small hump at about 153 °C relates to the rhombohedral– $Pnma$ orthorhombic phase transition. The depolarization temperature (T_d) of 91.5NBT–8.5KBT crystal is about 153 °C, which is higher than that (~120 °C) of Mn:94.6NBT–5.4BT crystal.⁷ Compared with

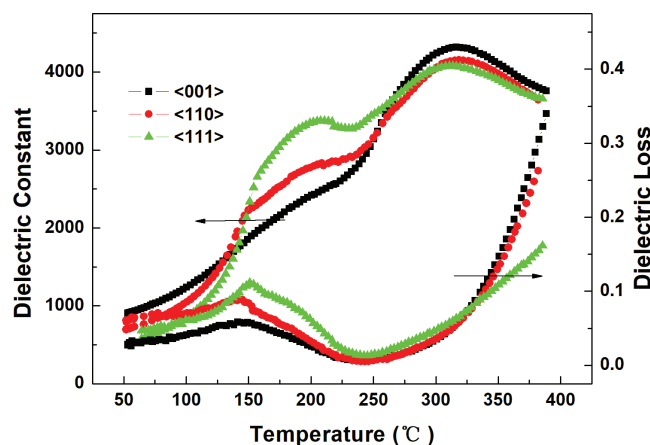


Fig. 2. Temperature dependences of dielectric constant and loss at 1 kHz for the 91.5NBT–8.5KBT crystal.

Mn:94.6NBT–5.4BT crystal, 91.5NBT–8.5KBT crystal owns wider operation temperatures in practical application. The depolarization mechanism has been discussed in detail in the previously published literature.¹³

Figure 3 shows the frequency dependences of dielectric constant and loss for 91.5NBT–8.5KBT crystal at room temperature. At 100 Hz, dielectric constant and loss are 690 and 0.020, 534 and 0.022, and 350 and 0.026 for <001>-, <110>-, and <111>-oriented 91.5NBT–8.5KBT crystals at 18 °C, which are listed in Table 1. The dielectric constant and loss show frequency dependence in the range of 100–800 Hz, and remain invariable in the range of 800–5000 Hz. The as-grown crystal exhibits relatively larger dielectric loss, which can be attributed to the presence of a space charge conduction mechanism. The space charge may result from bismuth V_{Bi}''' and oxygen V_o^{\cdot} vacancies, due to Bi_2O_3 volatility during crystal growth.³

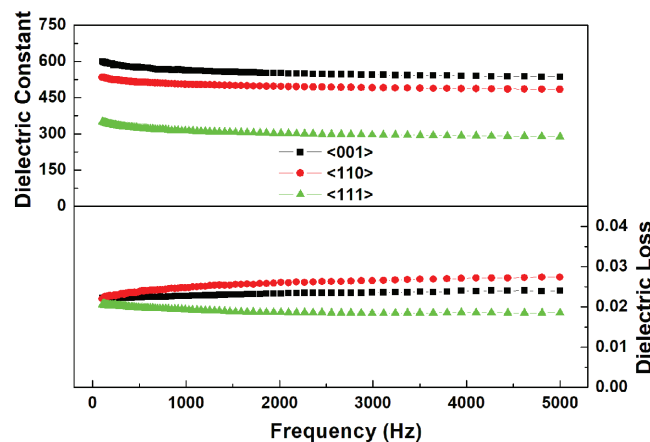


Fig. 3. Frequency dependences of dielectric constant and loss for the 91.5NBT–8.5KBT crystal at room temperature.

Table 1. Pyroelectric and dielectric parameters of poled 91.5NBT–8.5KBT single crystal and other lead-free materials at room temperature.

Material	Type	T_c (°C)	T_d (°C)	p ($\mu\text{C}/\text{m}^2 \cdot \text{K}$)	ε_r (@100 Hz)	$\tan\theta$ (@100 Hz)	F_i (pm/V)	F_v (m^2/C)	F_d ($\times 10^{-6} \text{Pa}^{-1/2}$)	Source
91.5NBT–8.5KBT <001>	Crystal	318	153	302	690	0.020	96.8	0.020	8.8	This work
91.5NBT–8.5KBT <110>	Crystal	319	153	504	534	0.022	161.5	0.040	18.7	This work
91.5NBT–8.5KBT <111>	Crystal	317	153	563	350	0.026	180.4	0.080	21.5	This work
Mn:94.6NBT–5.4BT <111>	Crystal	280	120	588	279	0.019	203.5	0.080	29.8	Ref. 7
PZT	Ceramic	315	—	350	471	0.005	109	0.026	24	Ref. 18
$[\text{Bi}_{0.5}(\text{Na}_{0.95}\text{K}_{0.05})_{0.05}]_{0.95}\text{-Ba}_{0.05}\text{TiO}_3$	Ceramic	—	—	325	853	0.028	194.6	0.026	13.4	Ref. 19

3.3. Pyroelectric properties at room temperature

Infrared detector made by pyroelectric material has many advantages, such as wide wavelength response, no requirement for cooling, high temperature stability, and high sensitivity. The pyroelectric coefficient (p) and figures of merits (FOMs) are important parameters for selecting the materials for pyroelectric applications. The FOMs include current responsivity $F_i = p/C_v$, voltage responsivity $F_v = p/(C_v \varepsilon_0 \varepsilon_r)$, and detectivity $F_d = p/[C_v(\varepsilon_0 \varepsilon_r \tan\theta)^{1/2}]$, where C_v , ε_0 , ε_r , and $\tan\theta$ are volume specific heat, permittivity of free space, dielectric constant, and dielectric loss, respectively.

The values of pyroelectric coefficient at 18°C are listed in Table 1. The pyroelectric coefficients are 3.02×10^{-4} , 5.04×10^{-4} , and $5.63 \times 10^{-4} \text{ C}/\text{m}^2 \cdot \text{K}$ for <001>-, <110>-, and <111>- oriented crystals. Similar to dielectric constant and loss, pyroelectric coefficient also shows obvious anisotropy. The <111>- oriented crystal possesses the highest p and the lowest ε_r . The value of p for <111>- oriented crystal is larger than those of the widely used pyroelectric materials such as LiTaO₃ crystal ($2.3 \times 10^{-4} \text{ C}/\text{m}^2 \cdot \text{K}$) and similar-composition Mn:82NBT–18KBT thick-film materials ($3.8 \times 10^{-4} \text{ C}/\text{m}^2 \cdot \text{K}$).^{14,15} Some literature works reported high pyroelectric coefficients for lead-free pyroelectric materials, such as $0.94(\text{Bi}_{0.5}\text{Na}_{0.5})\text{TiO}_3\text{-}0.06\text{Ba}(\text{Ti}_{0.75}\text{Zr}_{0.25})\text{O}_3$ ceramic ($27.20 \times 10^{-4} \text{ C}/\text{m}^2 \cdot \text{K}$)¹⁶ and Li-doped $\text{Ba}_{0.85}\text{Ca}_{0.15}\text{Ti}_{0.9}\text{Zr}_{0.1}\text{O}_3$ ceramic ($8.6 \times 10^{-4} \text{ C}/\text{m}^2 \cdot \text{K}$).¹⁷ However, low phase transition temperature (near room temperature) limits the practical application for these materials. The pyroelectric parameters of conventional pyroelectric material, representative lead-free single crystal, and similar-composition ceramics, such as PZT ceramic, Mn:NBT–KBT single crystal, and $[\text{Bi}_{0.5}(\text{Na}_{0.95}\text{K}_{0.05})_{0.05}]_{0.95}\text{-Ba}_{0.05}\text{TiO}_3$ ceramics, are listed in Table 1 as a comparison.^{18,7,19}

The dependency on the crystal orientation for pyroelectric properties can be considered as relating to the differences of spontaneous polarization direction and domain configuration.²⁰ The 91.5NBT–8.5KBT crystal is rhombohedral structure at room temperature, with spontaneous polarization along the <111>- direction. After poled along the polar axis, the <111>- oriented crystal approaches closely the

monodomain state and presents a largest remnant polarization, which results in the largest pyroelectric coefficient. The FOMs are calculated based on the above experimental results. The volume specific heat (C_v) is calculated to be $3.12 \times 10^6 \text{ J}/\text{m}^3 \cdot \text{K}$ on the basis of the specific heat per unit mass (C_p). These parameters are summarized in Table 1. At 18°C, F_i values are 96.8, 161.5, and 180.4 pm/V, F_v values are 0.02, 0.04, and 0.08 m^2/C , and F_d values are 8.8, 18.7, and 21.5 $\mu\text{Pa}^{1/2}$ for the <001>-, <110>-, and <111>- oriented 91.5NBT–8.5KBT crystals, respectively. Among the three crystallographic orientations, F_v and F_d of <111>- oriented crystals own the largest values, which are attributed to the largest pyroelectric coefficient and the lowest dielectric constant caused by domain configuration.²⁰

3.4. The influence of temperature and frequency on pyroelectric properties

In this work, the temperature and frequency dependences of pyroelectric properties of <001>-, <110>-, and <111>- oriented 91.5 NBT–8.5 KBT crystals were investigated. The p , F_d , and F_v were measured from 18°C to 103°C with the steps of $\Delta T = 5^\circ\text{C}$, which are shown in Fig. 4. From 18°C to 103°C, the pyroelectric coefficients increase by 10.6%, 9.9%, and 10.7% for the <001>-, <110>-, and <111>-oriented crystals, showing relatively high thermal stability. With the increase of the temperature, it can be seen from Fig. 4 that the F_v values gradually decrease, while the F_d values decrease at first, then increase at about 28°C, and finally, decrease again at 48°C. The variations of the F_v and F_d values can be attributed to the variations of dielectric constant and loss values with the increase of temperature, which may be related to the structural phase transition.

Instead of operating under various temperatures, the pyroelectric detectors made of pyroelectric materials need to operate under various frequencies. The frequency dependences of pyroelectric properties of 91.5NBT–8.5KBT crystal were also investigated. The frequency dependences of F_d and F_v for <001>-, <110>-, and <111>- oriented 91.5NBT–8.5KBT crystals are shown in Fig. 5. For the three crystallographic

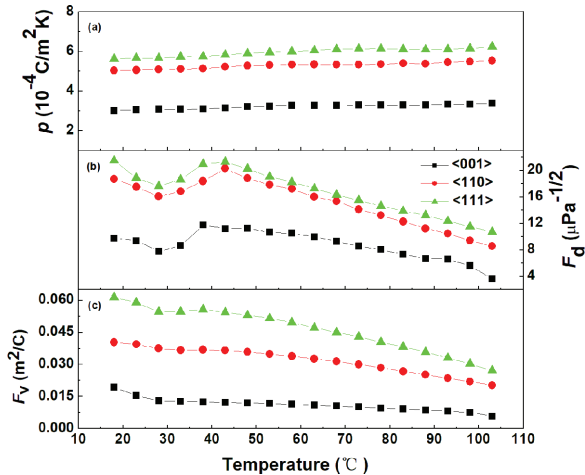


Fig. 4. Temperature dependences of p , F_d , and F_v for the $\langle 001 \rangle$ -, $\langle 110 \rangle$ -, and $\langle 111 \rangle$ -oriented crystals.

orientations of crystals, the F_d and F_v values slightly increase with the increase of the frequency from 100 Hz to 300 Hz, then remain invariable in the range of 300–4000 Hz.

4. Conclusions

In summary, the dielectric and pyroelectric properties of 91.5NBT–8.5KBT single crystal were investigated. The as-grown crystal exhibits obvious anisotropy. For the $\langle 111 \rangle$ orientation crystal, the value of ϵ_r is the lowest, while the values of p , F_d , and F_v are the largest among the three crystallographic orientations of crystals. The F_d and F_v exhibit weak frequency dependence in the range of 100–300 Hz. The pyroelectric coefficient increases with the increase of temperature from 18 °C to 103 °C, while the F_d and F_v values decrease in general from 18 °C to 103 °C. If the dielectric loss of the

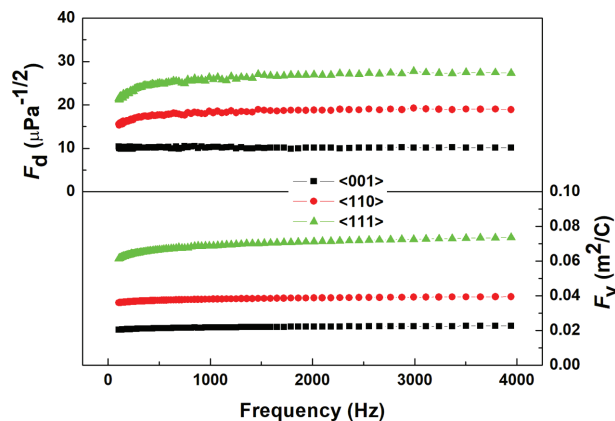


Fig. 5. Frequency dependences of figures of merit F_d and F_v for the $\langle 001 \rangle$ -, $\langle 110 \rangle$ -, and $\langle 111 \rangle$ -oriented crystals at room temperature.

as-grown crystal can be reduced, its pyroelectric properties will be optimized. So, further work on decreasing the dielectric loss deserves more attention.

Acknowledgments

This work was financially supported by the National Natural Science Foundation of China (NSFC Grant No. 51601101) and Natural Science Foundation of Ningbo (Grant No. 202003N4165).

References

- Y. Saito, H. Takao, T. Tani, T. Nonoyama, K. Takatori, T. Homma, T. Nagayu and M. Nakamura, Lead-free piezoceramics, *Nature (Lond.)* **432**, 84 (2004).
- W. F. Liu and X. B. Ren, Large piezoelectric effect in Pb-free ceramics, *Phys. Rev. Lett.* **103**, 257602 (2009).
- Q. H. Zhang, Y. Y. Zhang, F. F. Wang, Y. Wang, D. Lin, X. Zhao, H. S. Luo, W. W. Ge and D. Viehland, Enhanced piezoelectric and ferroelectric properties in Mn-doped $\text{Na}_{0.5}\text{Bi}_{0.5}\text{TiO}_3$ – BaTiO_3 single crystals, *Appl. Phys. Lett.* **95**, 102904 (2009).
- R. B. Sun, J. Z. Wang, F. Wang, T. F. Feng, F. Kong, X. Liu, Y. Li and H. S. Luo, Growth and electrical properties of $\text{Na}_{0.5}\text{Bi}_{0.5}\text{TiO}_3$ – $\text{K}_{0.5}\text{Bi}_{0.5}\text{TiO}_3$ lead-free single crystals by the TSSG method, *Ceram. Int.* **42**, 14557 (2016).
- H. F. Zhou, H. Deng, X. Liu, H. Yan, X. Y. Zhao, H. S. Luo and J. Xu, Dielectric and piezoelectric properties of lead-free $(\text{K}_{0.44}\text{Na}_{0.46})\text{NbO}_3$ –0.5% MnO_2 single crystals grown by the TSSG method, *Ceram. Int.* **42**, 15327 (2016).
- A. M. Balakt, C. P. Shaw and Q. Zhang, The effects of Ba^{2+} content on depolarization temperature and pyroelectric properties of lead-free $0.94\text{Na}_{0.5}\text{Bi}_{0.5}\text{TiO}_3$ – $0.06\text{Ba}_{1+x}\text{TiO}_3$ ceramics, *J. Mater. Sci., Mater. Electron.* **27**, 12947 (2016).
- R. B. Sun, J. Z. Wang, F. Wang, T. Feng, Y. Li, Z. Chi, X. Zhao and H. S. Luo, Pyroelectric properties of Mn-doped $94.6\text{Na}_{0.5}\text{Bi}_{0.5}\text{TiO}_3$ – 5.4BaTiO_3 lead-free single crystals, *J. Appl. Phys.* **115**, 074101 (2014).
- M. Aggarwal, M. Kumar, R. Syal, V. P. Singh, A. K. Singh, S. Dhiman and S. Kumar, Enhanced pyroelectric figure of merits in Sr and Zr co-doped porous BaTiO_3 ceramics, *J. Mater. Sci., Mater. Electron.* **31**, 2337 (2020).
- Z. Abdelkafifi, N. Abdelmoula, H. Khemakhem and M. El Marssi, Pyroelectric and dielectric properties of lead-free $\text{BaTi}_{0.925}(\text{Yb}_{0.85}\text{Fe}_{0.15})_{0.5}\text{Nb}_{0.5}\text{O}_3$ ceramic, *J. Mater. Sci., Mater. Electron.* **32**, 2441 (2021).
- L. E. Garn and E. J. Sharp, Use of low-frequency sinusoidal temperature waves to separate pyroelectric currents from non-pyroelectric currents: Part I: Theory, *J. Appl. Phys.* **53**, 8974 (1982).
- V. Dorcet, G. Trolliard and P. Boullay, Reinvestigation of phase transitions in $\text{Na}_{0.5}\text{Bi}_{0.5}\text{TiO}_3$ by TEM: Part I: First order rhombohedral to orthorhombic phase transition, *Chem. Mater.* **20**, 5061 (2008).
- G. Trolliard and V. Dorcet, Reinvestigation of phase transitions in $\text{Na}_{0.5}\text{Bi}_{0.5}\text{TiO}_3$ by TEM: Part II: Second order orthorhombic to tetragonal phase transition, *Chem. Mater.* **20**, 5074 (2008).
- R. B. Sun, X. Li, Q. Zhang, B. Fang, H. Zhang, H. Zhang, D. Lin, S. Wang, X. Y. Zhao and H. S. Luo, Growth and orientation dependence of electrical properties of $0.92\text{Na}_{0.5}\text{Bi}_{0.5}\text{TiO}_3$ – $0.08\text{K}_{0.5}\text{Bi}_{0.5}\text{TiO}_3$ lead-free piezoelectric single crystal, *J. Appl. Phys.* **109**, 124113 (2011).
- B. M. Kulwicki, A. Amin, H. R. Beratan and C. M. Hanson, Pyroelectric imaging, *Proc. Eighth IEEE Int. Symp. Applications of Ferroelectrics* (1992), pp. 1–10.

- ¹⁵H. Zhang, S. Jiang and K. Kajiyoshi, Pyroelectric and dielectric properties of Mn modified $0.82\text{Bi}_{0.5}\text{Na}_{0.5}\text{TiO}_3-0.18\text{Bi}_{0.5}\text{K}_{0.5}\text{TiO}_3$ lead-free thick films, *J. Am. Ceram. Soc.* **92**, 2147 (2009).
- ¹⁶M. Shen, W. Li, M. Y. Li, H. Liu, J. Xu, S. Qiu, G. Zhang, Z. Lu, H. Li and S. Jiang, High room-temperature pyroelectric property in lead-free BNT-BZT ferroelectric ceramics for thermal energy harvesting, *J. Eur. Ceram. Soc.* **39**, 1810 (2019).
- ¹⁷X. Liu, Z. Chen, D. Wu, B. Fang, J. Ding, X. Zhao, H. Xu and H. Luo, Enhancing pyroelectric properties of Li-doped $(\text{Ba}_{0.85}\text{Ca}_{0.15})$ $(\text{Zr}_{0.1}\text{Ti}_{0.9})\text{O}_3$ lead-free ceramics by optimizing calcination temperature, *Jpn. J. Appl. Phys.* **54**, 071501 (2015).
- ¹⁸T. Takenaka and K. Sakata, Pyroelectric properties of grain-oriented bismuth layer-structured ferroelectric ceramics, *Jpn. J. Appl. Phys.* **22**, 53 (1983).
- ¹⁹S. T. Lau, C. H. Cheng, S. H. Choy, D. M. Lin, K. W. Kwok and H. L. W. Chan, Lead-free ceramics for pyroelectric applications, *J. Appl. Phys.* **103**, 104105 (2008).
- ²⁰S.-E. Park and T. R. ShROUT, Ultrahigh strain and piezoelectric behavior in relaxor based ferroelectric single crystals, *J. Appl. Phys.* **82**, 1804 (1997).